

- Supplemental information -

Fabrication of Phosphorylated Graphene Oxide-Chitosan Composite for Highly Effective and Selective Capture of U(VI)

Yawen Cai,^{abc} Chunfang Wu,^{abc} Zhiyong Liu,^{abc} Linjuan Zhang,^d Lanhua Chen,^{abc} Jianqiang Wang,^d Xiangke Wang,^{abe} Shitong Yang,*^{abc} Shuaowang Wang*^{abc}

^a School for Radiological and Interdisciplinary Sciences (RAD-X), Soochow University, 215123, Suzhou, P. R. China

^b Collaborative Innovation Center of Radiation Medicine of Jiangsu Higher Education Institutions, 215123, Suzhou, P. R. China

^c Jiangsu Provincial Key Laboratory of Radiation Medicine and Protection, 215123, Suzhou, P. R. China

^d Shanghai Institute of Applied Physics and Key Laboratory of Nuclear Radiation and Nuclear Energy Technology, Chinese Academy of Sciences, 201800, Shanghai, P. R. China

^e School of Environment and Chemical Engineering, North China Electric Power University, Beijing 102206, P. R. China

*Corresponding authors. Email: shitongyang@suda.edu.cn (S. YANG); shuaowang@suda.edu.cn (S. WANG); Tel: [+86-512-65883945](tel:+86-512-65883945); Fax: [+86-512-65883945](tel:+86-512-65883945).

Contents:

S1 FTIR spectra (Figure S1)

S2 Sorption capacity (Tables S1 and S2)

S3 Selectivity (Table S3)

S4 Desorption experiments

S5 XAS analysis (Figure S2, Table S4)

S6 XPS analysis (Table S5)

S1 FTIR spectra

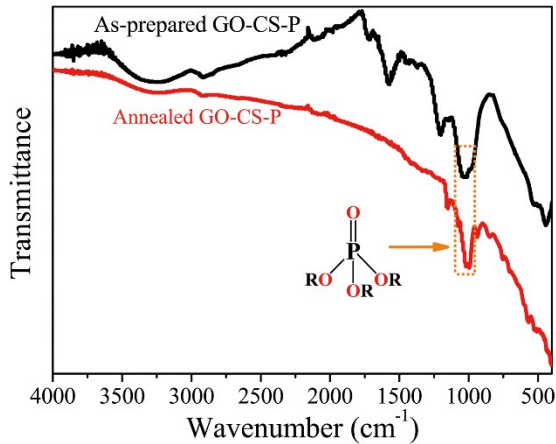


Figure S1. FTIR spectra of as-prepared and annealed GO-CS-P.

S2 Sorption capacity

The sorption isotherms of U(VI) on GO, GO-CS and GO-CS-P were respectively simulated using the Langmuir and Freundlich models as described below:^{S1}

$$\text{Langmuir model: } q_e = \frac{K_L q_{\max} C_e}{1 + K_L C_e} \quad (1)$$

$$\text{Freundlich model: } q_e = K_F C_e^n \quad (2)$$

Herein, q_e (mg/g) is the equilibrium U(VI) adsorption amount on per weight unit of the adsorbent, C_e (mg/L) is the residual U(VI) concentration after adsorption equilibrium, K_L is the Langmuir coefficient, K_F is the Freundlich coefficient, q_{\max} (mg/g) is the maximum amount for U(VI) adsorbed onto the GO, GO-CS or GO-CS-P, which for Langmuir adsorption would correspond to a monolayer, and n is the Freundlich exponent. The parameters derived from the model fitting are listed in Table S1. Based on the correlation coefficient (R^2) values, the sorption isotherm data are better fitted by the Langmuir equation for all the three adsorbents. This phenomenon implies that the captured of U(VI) by GO, GO-CS or GO-CS-P are chemisorption processes.^{S2-S4} Note that the sorption isotherm experiments were conducted at a constant solid dosage of 0.05 g/L. A finite amount of surface sites would be provided for binding U(VI), resulting in the appearance of a saturated sorption amount at higher U(VI) concentration. In this case, the sorption isotherm would not be well simulated by the Freundlich model, which assumes an exponential rising of U(VI) sorption amount with the increase of its initial concentration in solution. The n values of the Freundlich model are calculated to be

smaller than 1, indicating the occurrence of a nonlinear sequestration process of U(VI) on GO, GO-CS and GO-CS-P.

Table S1 Parameters for Langmuir and Freundlich model fits at 293 K.

	Parameters	GO	GO-CS	GO-CS-P
Langmuir	q_{\max} (mg/g)	573.91	346.16	779.44
	K_L (L/mg)	0.240	0.149	0.100
	R^2	0.991	0.981	0.991
Freundlich	K_F (mg ¹⁻ⁿ L ⁿ /g)	167.68	94.40	200.68
	n	0.267	0.264	0.273
	R^2	0.958	0.972	0.973

Blank test: The blank experiment was conducted in the absence of adsorbents by ranging the initial U(VI) concentration from 5.0×10^{-5} to 7.5×10^{-4} mol/L. Specifically, the NaNO₃ electrolyte solution and U(VI) stock solution were added into a series of polyethylene centrifuge tubes to achieve the desired concentrations. The pH values were adjusted to 5.0 by adding a negligible volume of HNO₃ and/or NaOH solutions. Then, the centrifuge tubes were gently oscillated for 24 h, which was the same as that in the batch uptake experiments. Afterwards, the solution was filtrated with 0.22 μ m filter membrane and the concentration of U(VI) in the filtrate was measured by using inductively coupled plasma-atomic emission spectrometry (ICP-AES). According to the measurement, the final concentration of U(VI) was almost equal to its initial concentration. This result eliminated the potential precipitation of U-containing solid phases due to hydrolysis.

Table S2 Comparison of U(VI) sorption capacity of GO-CS-P with other adsorbents.

Materials	Experimental conditions	q_{\max} (mg/g)	References
MWCNTs	pH=5.0, $T=298$ K	24.9	[S5]
Oxime-CMK-5	pH=4.5, $T=298$ K	65.18	[S6]
GO-CNTs	pH=5.0, $T=298$ K	100	[S7]
UiO-66	pH=5.5, $T=287$ K	109.9	[S8]
UiO-66-NH ₂	pH=5.5, $T=287$ K	114.9	[S8]
AMGO	pH=5.9, $T=298$ K	141.2	[S9]
COF-HBI	pH=4.5, $T=298$ K	211	[S10]
UiO-68-P(O)(OEt) ₂	pH=2.5, $T=298$ K	217	[S11]
CTPP	pH=5.0, $T=298$ K	236.9	[S12]
MOF-76	pH=3.0, $T=298$ K	298	[S13]
Zr _{1-x} Ti _x P ₂ O ₇	pH=5.0, $T=303$ K	309.8	[S14]
NiCo ₂ O ₄ @rGO	pH=5.0, $T=298$ K	333.3	[S15]
FJSM-SnS	pH=4.1, $T=298$ K	338.43	[S16]
GO-CS	pH=5.0, $T=293$ K	346.16	This work
MIL-101-DETA	pH=5.5, $T=298$ K	350	[S17]
AGH	pH=6.0, $T=298$ K	398.4	[S18]
APSS	pH=5.3, $T=298$ K	409	[S19]
Ca-Mg-Al-LDO ₅₀₀	pH=5.0, $T=298$ K	486.8	[S20]
GO nanosheets	pH=5.0, $T=293$ K	573.91	This work
GO-CS-P	pH=5.0, $T=293$ K	779.44	This work

S3 Selectivity

Table S3 Selectivity coefficients of U(VI) with regard to each competing cation for binding on GO, GO-CS and GO-CS-P.

Adsorbents	pH	$K_{S_M^U}$						
		Cs(I)	Sr(II)	Co(II)	Cd(II)	La(III)	Eu(III)	Yb(III)
GO	5.0	4.94	2.75	3.48	3.23	2.53	2.26	2.65
GO-CS	5.0	4.32	1.77	2.35	1.88	1.49	1.44	1.56
GO-CS-P	5.0	∞	8.69	10.54	7.16	6.47	5.60	5.79

S4 Desorption experiments

The desorption experiments were conducted by soaking two parallel U(VI)-bound GO-CS-P samples in 200 mL of the $\text{CH}_3\text{COONH}_4$ (5.0×10^{-3} mol/L, 100 times higher than the initial U(VI) concentration of 5.0×10^{-5} mol/L) and HNO_3 solution (0.01 mol/L), respectively. After 2 days, the suspensions were centrifuged and filtered through 0.22 μm filter membranes. The amounts of released U(VI) were measured by ICP-AES.

S5 XAS analysis

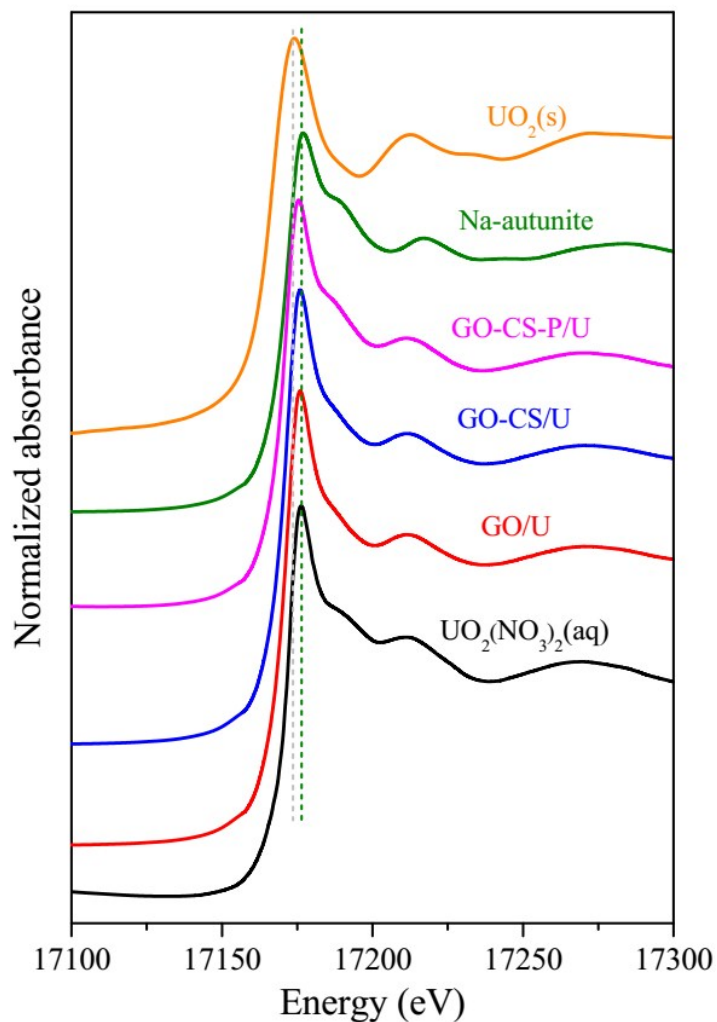


Figure S2. XANES spectra of U-containing reference and uptake samples.

Table S4 Structural parameters derived from EXAFS analysis for U-containing samples.

Sample	Shell	R (Å)	CN	σ^2 (Å ²)
UO ₂ (NO ₃) ₂ (aq)	U-O _{ax}	1.781(2)	2.0*	0.0025(3)
	U-O _{eq}	2.348(4)	3.9(2)	0.0038(2)
GO/U	U-O _{ax}	1.784(1)	2.0*	0.0034(4)
	U-O _{eq}	2.355(4)	3.8(3)	0.0046(3)
	U-C	2.913(4)	1.8(4)	0.0055(5)
GO-CS/U	U-O _{ax}	1.779(3)	2.0*	0.0028(4)
	U-O _{eq}	2.348(5)	3.7(2)	0.0041(2)
	U-N	2.396(3)	0.9(4)	0.0044(5)
	U-C	2.907(4)	1.3(5)	0.0067(6)
GO-CS-P/U	U-O _{ax}	1.778(2)	2.0*	0.0035(2)
	U-O _{eq}	2.350(3)	3.9(1)	0.0046(4)
	U-C	2.898(4)	1.0(3)	0.0055(5)
	U-P1	3.124(3)	2.1(2)	0.0074(4)
	U-P2	3.610(4)	1.3(2)	0.0102(5)
Na-autunite	U-O _{ax}	1.778(2)	2.0*	0.0036(3)
	U-O _{eq}	2.352(3)	3.8(3)	0.0041(4)
	U-P	3.595(4)	4.1(1)	0.0058(2)
	U-U	5.233(2)	3.9(2)	0.0138(6)

R--Bond distance, CN--Coordination number, σ^2 --Debye-Waller factor, *--Fixed or constrained during spectral fitting. The estimated standard deviations are listed in parentheses, representing the error in the last digit.

S6 XPS analysis

Table S5 Binding energies of P 2p, O 1s and U 4f before and after U(VI) uptake by GO-CS-P.

Samples	Valence states							
	P 2p (eV)		O 1s (eV)			U 4f (eV)		
	P 2p _{3/2}	P 2p _{1/2}	O-C=O	P-O	C-O-C	-OH	U 4f _{7/2}	U 4f _{5/2}
Before U(VI) uptake	133.57	134.57	531.33	532.36	533.21	533.95	---	---
After U(VI) uptake	133.42	134.32	531.35	532.03	532.92	533.40	380.27	382.07
							391.10	392.88

References

- S1 P. M. Abraham, S. Barnikol, T. Baumann, M. Kuehn, N. P. Ivleva and G. E. Schaumann, *Environ. Sci. Technol.*, 2013, **47**, 5083-5091.
- S2 L. Zhou, Y. Wang, Z. Liu and Q. Huang, *J. Hazard. Mater.*, 2009, **161**, 995-1002.
- S3 S. Yang, P. Zong, J. Hu, G. Sheng, Q. Wang, X. Wang, *Chem. Eng. J.*, 2013, **214**, 376-385.
- S4 Y. Cai, F. Yuan, X. Wang, Z. Sun, Y. Chen, Z. Liu, X. Wang, S. Wang, S. Yang, *Cellulose*, 2017, **24**, 175-190.
- S5 I. I. Fasfous, J. N. Dawoud, *Appl. Surf. Sci.*, 2012, **259**, 433-440.
- S6 G. Tian, J. Geng, Y. Jin, C. Wang, S. Li, Z. Chen, H. Wang, Y. Zhao, S. Li, *J. Hazard. Mater.*, 2011, **190**, 442-450.
- S7 Z. Gu,; Y. Wang, J. Tang, J. Yang, J. Liao, Y. Yang, N. Liu, *J. Radioanal. Nucl. Chem.*, 2015, **303**, 1835-1842.
- S8 B. Luo, L. Yuan, Z. Chai, W. Shi, Q. Tang, *J. Radioanal. Nucl. Chem.*, 2016, **307**, 269-276.
- S9 L. Chen, D. Zhao, S. Chen, X. Wang, C. Chen, *J. Colloid Interface Sci.*, 2016, **472**, 99-107.
- S10 J. Li, X. Yang, C. Bai, Y. Tian, B. Li, S. Zhang, X. Yang, S. Ding, C. Xia, X. Tan, L. Ma, S. Li, *J. Colloid Interface Sci.*, 2015, **437**, 211-218.
- S11 M. Carboni, C. W. Abney, S. Liu, W. Lin, *Chem. Sci.*, 2013, **4**, 2396-2402.
- S12 M. K. Sureshkumar, D. Das, M. B. Mallia, P. C. Gupta, *J. Hazard. Mater.*, 2010, **184**, 65-72.
- S13 W. Yang, Z. Bai, W. Shi, L. Yuan, T. Tian, Z. Chai, H. Wang, Z. Sun, *Chem. Commun.*, 2013, **49**, 10415-10417.
- S14 R. Wang, J. Ye, A. Rauf, X. Wu, H. Liu, G. Ning, H. Jiang, *J. Hazard. Mater.*, 2016, **315**, 76-85.
- S15 X. Song, L. Tan, X. Sun, H. Ma, L. Zhu, X. Yi, Q. Dong, J. Gao, *Dalton Trans.*, 2016, **45**, 16931-16937.
- S16 M. Feng, D. Sarma, X. Qi, K. Du, X. Huang, M. G. Kanatzidis, *J. Am. Chem. Soc.*, 2016, **138**, 12578-12585.
- S17 Z. Bai, L. Yuan, L. Zhu, Z. Liu, S. Chu, L. Zheng, J. Zhang, Z. Chai, W. Shi, *J. Mater. Chem. A*, 2015, **3**, 525-534.
- S18 F. Wang, H. Li, Q. Liu, Z. Li, R. Li, H. Zhang, L. Liu, G. A. Emelchenko, J. Wang, *Sci. Rep.*, 2016, **6**, 16367.
- S19 Y. Liu, L. Yuan, Y. Yuan, J. Lan, Z. Li, Y. Feng, Y. Zhao, Z. Chai, W. Shi, *J. Radioanal. Nucl. Chem.*, 2012, **292**, 803-810.
- S20 Y. Zou, X. Wang, F. Wu, S. Yu, Y. Hu, W. Song, Y. Liu, H. Wang, T. Hayat, X. Wang, *ACS Sustainable Chem. Eng.*, 2017, **5**, 1173-1185.